Available online at www.sciencedirect.com
ScienceDirect
Journal of Power Sources 177 (2008) 323–329
JOURNAL OF POWER SOURCES
www.elsevier.com/locate/jpowsour

Solid-oxide fuel cell operated on in situ catalytic decomposition products of liquid hydrazine

Hongxia Gu [a], Ran Ran [a,*], Wei Zhou [a], Zongping Shao [a,**], Wanqin Jin [a], Nanping Xu [a], Jeongmin Ahn [b]

[a] *State Key Laboratory of Materials-Oriented Chemical Engineering, Nanjing University of Technology, No. 5 Xing Mofan Road, Nanjing, JiangSu 210009, PR China*
[b] *School of Mechanical and Materials Engineering, Washington State University, Sloan 217, Pullman, WA 99164-2920, USA*

Received 21 September 2007; received in revised form 13 November 2007; accepted 13 November 2007
Available online 26 November 2007

Abstract

Hydrazine was examined as a fuel for a solid-oxide fuel cell (SOFC) that employed a typical nickel-based anode. An in situ catalytic decomposition of hydrazine at liquid state under room temperature and ambient pressure before introducing to the fuel cell was developed by applying a $Ba_{0.5}Sr_{0.5}Co_{0.8}Fe_{0.2}O_{3-\delta}$ (BSCF) oxide catalyst. Catalytic testing demonstrated that liquid N_2H_4 can be decomposed to gaseous NH_3 and H_2 at a favorable rate and at a temperature as low as 20 °C and H_2 selectivity reaching values as high as 10% at 60 °C. Comparable fuel cell performance was observed using either the in situ decomposition products of hydrazine or pure hydrogen as fuel. A peak power density of ~850 mW cm^{-2} at 900 °C was obtained with a typical fuel cell composed of scandia-stabilized zirconia and $La_{0.8}Sr_{0.2}MnO_3$ cathode. The high energy and power density, easy storage and simplicity in fuel delivery make it highly attractive for portable applications.

Keywords: Solid-oxide fuel cell; Hydrazine; $Ba_{0.5}Sr_{0.5}Co_{0.8}Fe_{0.2}O_{3-\delta}$; Nickel; Portable application

1. Introduction

A fuel cell is an electrochemical energy conversion device that is known for its high energy efficiency and low environmental impact. Its high energy density and quick "recharging" (refueling) capability in connection with the increased power requirements of portable devices have resulted in considerable interest in fuel cells for use in portable and micropower applications. A solid-oxide fuel cell (SOFC) is an all-solid high-temperature fuel cell that applies a conducting (oxygen ion or proton) oxide as the electrolyte [1,2]. Traditionally, SOFCs were not seriously considered for mobile applications. However, recent advances in micro-tubular and single-chamber SOFCs have changed this situation [3–10]. The significant advantages of SOFCs over polymer–electrolyte membrane fuel cells (PEMFCs) for portable applications arise from its versatile fuel selection coupled with higher power density. Hydrogen, carbon monoxide, hydrocarbons, alcohols and ammonia are all potential fuels for SOFCs [11–13].

As the ideal fuel for portable fuel cell, it should meet several requirements: high energy density, easy storage, good availability and favorable electrochemical activity. Liquid fuels are preferred over compressed hydrogen due to the fact that they have much higher energy density per volume. On the other hand, state-of-the-art fuel cell materials are the most attractive components for portable SOFCs since their properties are well established. Stabilized zirconia–Ni and doped ceria–Ni cermets are the typical anodes for SOFCs. The nickel functions as the conduction path for electrons and also the catalyst for the electrochemical oxidation of hydrogen. Liquid hydrocarbons have recently attracted considerable attention as potential fuels for SOFCs due to their high energy density and good availability [14–17]. However, with the liquid hydrocarbons serious carbon coking was observed over the

* Corresponding author. Tel.: +86 25 83587722; fax: +86 25 83365813.
** Corresponding author at: State Key Laboratory of Materials-Oriented Chemical Engineering, Nanjing University of Technology, College of Chemistry & Chemical Engineering, No. 5 Xing Mofan Road, Nanjing, JiangSu 210009, PR China. Tel.: +86 25 83587722; fax: +86 25 83365813.
E-mail addresses: ranrandalian@yahoo.com (R. Ran), shaozp@njut.edu.cn (Z. Shao).

0378-7753/$ – see front matter © 2007 Elsevier B.V. All rights reserved.
doi:10.1016/j.jpowsour.2007.11.062

nickel anode [17]. Although considerable advances have been made with both CeO_2–Cu and perovskite anodes [18–21], the relatively low power density and the difficulty in fuel cell fabrication with the use of those materials have introduced new problems.

Hydrazine, or diamine, in the form of propellant for thrusters, is by far the most common means of spacecraft propulsion and attitude control. And it is used as a monopropellant for satellite station-keeping motors because hydrazine will decompose (ignite) when placed in contact with platinum group metal catalysts. Hydrazine monopropellant systems have also been used as auxiliary power units on aircraft.

In this paper, liquid hydrazine was applied as the fuel for the SOFC. Hydrazine fuel cells were investigated extensively in the 1960–1970s, as an alkaline fuel cell (AFC) that utilized a liquid alkaline electrolyte [22–24]. Recently, the possible application of hydrazine as the fuel for a fuel cell based on a polymer–electrolyte membrane was also reported [25–27]. However, the application of hydrazine as fuel for SOFCs is rarely reported in literature. Here an in situ decomposition of liquid hydrazine to gaseous NH_3 and H_2 at room temperature and ambient pressure by applying an innovative oxide catalyst before introducing it into the fuel cell reactor was proposed. When compared to using hydrogen as a fuel based on a typical nickel-based anode-supported SOFC, comparable performance was obtained. The in situ decomposition of liquid hydrazine to form gaseous products does not require a fuel pump or a high-pressure gas tank and valves, which greatly simplifies the fuel cell system.

2. Experimental

2.1. Catalyst preparation

$Ba_{0.5}Sr_{0.5}Co_{0.8}Fe_{0.2}O_{3-\delta}$ (BSCF) oxide was used as the catalyst for the liquid state hydrazine decomposition at room temperature. BSCF powders were synthesized by a combined EDTA–citrate complexing sol–gel process [28]. Stoichiometric amounts of $Ba(NO_3)_2$, $Sr(NO_3)_2$, $Co(NO_3)_2$, and $Fe(NO_3)_3$ were dissolved in water, followed by the addition of EDTA–$NH_3{\cdot}H_2O$ and citric acid in sequence at the mole ratio of EDTA:citric acid:metal ions = 1:2:1. $NH_3{\cdot}H_2O$ was applied during the evaporation of the water in order to sustain a pH value of around 6 for the solution. A gel was finally obtained, which was pre-fired at 250 °C for 2 h and further calcined at 800–1000 °C for 5 h to result in the final product with the desired composition.

2.2. Fuel cell fabrication

An anode-supported thin-film electrolyte fuel cell with $NiO + Sc_{0.1}Zr_{0.9}O_{1.9}$ (scandia-doped zirconia, ScSZ) anode, ScSZ electrolyte, and $La_{0.8}Sr_{0.2}MnO_3$ (LSM) cathode were applied in this study. Commercial NiO (Shanghai Hengxin Chemical Reagent Co. Ltd.) was applied for the nickel source. ScSZ and LSM were synthesized by the EDTA–citrate combined complexing process similar to the preparation of BSCF. The anode materials were prepared by mixing NiO and ScSZ powders in the ratio of 60:40 (wt.%) using a high-energy ball miller (FRITSCH, Pulverisette 6). A bi-layer of ScSZ electrolyte and anode support was co-pressed into disks of 15 mm in diameter and then co-fired at 1500 °C in air for 5 h. The subsequent layer of LSM with an effective area of 0.48 cm^2 was spray deposited onto the surface of the electrolyte and then sintered at 1150 °C in air for 2 h.

2.3. Hydrazine catalytic decomposition test

The catalytic activity of BSCF for the hydrazine decomposition was tested between 20 and 65 °C using a flat bottom flask, as shown in Fig. 1. 0.5 g of the BSCF catalyst was dropped into 30 mL of N_2H_4 liquid in a 250 mL flat bottom flask, which was stirred strongly with a magnetic stirrer and heated with a water bath to ensure a homogeneous temperature distribution of the hydrazine during the exothermal hydrazine decomposition. Gaseous products were first introduced to a H_3PO_4 trap to get rid of N_2H_4 vapor and NH_3. The formation rate of $N_2 + H_2$ was then measured by the volumetric method. The ratio of N_2 and H_2 in the effluent gas was also in situ measured by GC (Varian 3800) equipped with a 5 Å molecule sieve column for composition analysis.

2.4. Fuel cell test

The fuel cell test was performed in a self-constructed SOFC test station. Silver paste was applied as the current collector for both the cathode and anode. The cell was sealed onto a quartz tube with the cathode side open to ambient air. Hydrogen at the flow rate of 80 mL min^{-1} [STP] with the help of mass flow controller, or the in situ decomposed product of hydrazine, was introduced to the anode as the fuel. A Keithley 2420 source meter was used for the *I–V* polarization test. Four-terminal configuration was employed.

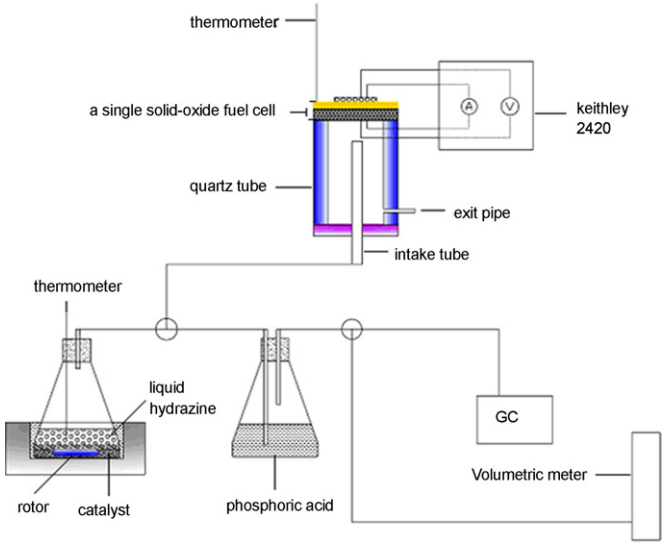

Fig. 1. The diagram of test device.

2.5. Other characterization

The phase composition of BSCF and other fuel cell components were examined by X-ray diffraction (XRD, Bruker D8 Advance) equipped with Cu Kα radiation. The experimental diffraction patterns were collected at room temperature by step scanning at the range of $20^\circ \leq \theta \leq 80^\circ$. The specific surface area of the BSCF catalyst was characterized by N_2 adsorption using a BELSORP II instrument at the temperature of liquid nitrogen. The morphological properties of the fuel cell were examined by environmental scanning microscopy (ESEM, QUANTA-2000). The electrode performance was investigated by the ac impedance method using an electrochemical workstation based on Solartron 1287 potentiostat and a 1260 A frequency response analyzer. The applied frequency ranged from 0.01 Hz to 10 kHz with signal amplitude of 10 mV under open cell voltage (OCV) conditions.

3. Results and discussion

BSCF is a mixed oxygen ionic and electronic conductor, which has been widely applied as the ceramic membrane for separation of oxygen from air and more recently as the cathode for intermediate-temperature SOFCs with high performance [29,30]. Mixed conducting oxides have also been found to be excellent catalysts for the decomposition of H_2O_2 to H_2O and O_2 in liquid state [31]. Since N_2H_4 has a similar molecular structure to H_2O_2, the catalytic activity of BSCF for N_2H_4 decomposition was investigated. Blank runs demonstrated that no thermal decomposition of hydrazine occurred at a temperature lower than 100 °C. This suggests that hydrazine by itself is stable enough as a fuel. Zheng et al. also observed that hydrazine decomposed only slightly at a temperature lower than 170 °C and 100% conversion was reached only at temperature higher than ~250 °C [32]. After the calcination in air at 1000 °C, the typical cubic perovskite structure was observed for BSCF, suggesting the formation of the desired phase structure. BET surface area of the oxide was found to be only 0.48 $m^2\,g^{-1}$. Such low surface area is due to the high surface activity of BSCF [30] and the high calcination temperature (1000 °C). After dropping the catalyst into the liquid hydrazine, gaseous products immediately evolved from the catalyst surface, demonstrating the high activity of BSCF towards the hydrazine decomposition. The formation rate of the gaseous products was found to increase quickly with higher operation temperatures. At temperatures higher than 65 °C, too much heat produced during the hydrazine decomposition led to the out of control of temperature.

With the molecular structure of N_2H_4, there are two types of bonds available, N–N and N–H. Therefore, the catalytic decomposition can proceed in two different ways:

$$N_2H_4 \rightarrow N_2 + 2H_2 \quad (\Delta H = -95.4\,\text{kJ mol}^{-1}) \tag{1}$$

$$3N_2H_4 \rightarrow N_2 + 4NH_3 \quad (\Delta H = -157.4\,\text{kJ mol}^{-1}) \tag{2}$$

The overall decomposition can be expressed as follows:

$$3N_2H_4 \rightarrow 4(1-x)NH_3 + (1+2x)N_2 + (6x)H_2 \tag{3}$$

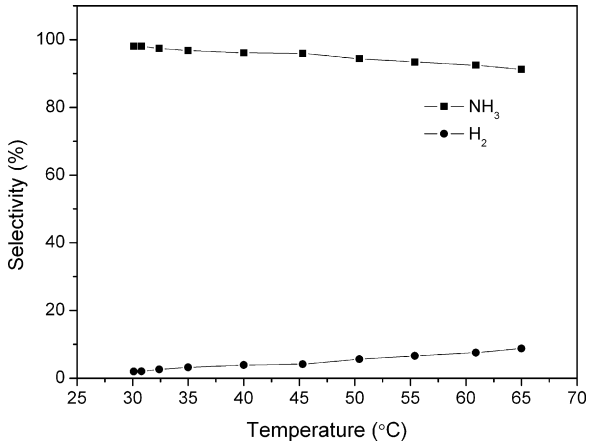

Fig. 2. The selectivity of H_2 and NH_3 under different temperature.

The H_2 selectivity (towards the reaction (1)), x can be calculated by

$$x = \frac{1/2[H_2]}{1/2[H_2] + 3/4[NH_3]} = \frac{2[H_2]}{2[H_2] + 3[NH_3]} \tag{4}$$

The measured temperature dependence of H_2 and NH_3 selectivity is shown in Fig. 2. It indicates that the catalytic decomposition of N_2H_4 over the BSCF catalyst favored both the cracking of N–N and N–H bonds, but with the main reaction more towards the N–N cracking to form NH_3 and N_2. The H_2 selectivity was found to increase monotonically with the increase in operating temperature at the investigated range of 20–65 °C. The reaction at temperatures higher than 65 °C was too fast; therefore no further investigation was conducted. The hydrogen selectivity reached ~10% at 60 °C with the BSCF catalyst. In the molecular structure of N_2H_4, the bonding energy for N–N and N–H is 60 kJ mol^{-1} and 84 kJ mol^{-1}, respectively. This suggests that the N–H bond in N_2H_4 thermodynamically is more stable than the N–N bond. In other words, the decomposition thermodynamically prefers the N–N cracking to form NH_3 and N_2. Indeed, it was reported that below 300 °C, the reaction was 100% towards the formation of N_2 and NH_3 over typical Ir/Al_2O_3 catalyst [33]. The formation of hydrogen suggests that the BSCF catalyst also favored the cracking of the N–H bond. It is surmised that the N–H bond in the N_2H_4 structure was likely activated by the formation of the hydrogen–oxygen bond via its hydrogen interacting with the surface oxygen ions in the BSCF perovskite. The formation of the O–H bond weakened the bonding strength for the N–H in N_2H_4 and made the cracking of the N–H bond favorable. An investigation of the activation mechanism of perovskite for the N_2H_4 decomposition is definitely required and will be conducted in the future.

In the test of the hydrazine decomposition rate, gas evolved from the flask was then introduced to a H_3PO_4 trap for the absorption of the NH_3 gas and the minor amount of N_2H_4 vapor in the gaseous products. The purified gas was then connected with a volumetric meter for measuring the formation rate of $N_2 + H_2$. Based on the results from volumetric experiments together with the selectivity of H_2 and NH_3 as detected by GC (Fig. 2), the N_2H_4 decomposition rate and the formation rates

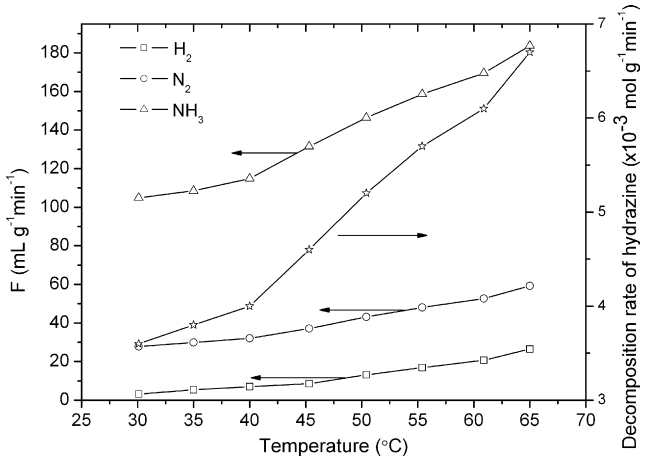

Fig. 3. H_2/NH_3 production rates and N_2H_4 decomposition rate.

of H_2, NH_3 and N_2 were then calculated. As shown in Fig. 3, favorable N_2H_4 decomposition and H_2/NH_3 production rates were observed. The electrical power generated from the in situ created H_2/NH_3 fuels per gram of catalyst at various temperatures was then calculated (Fig. 4). It was found that 1 g of BSCF catalyst was able to produce enough H_2/NH_3 fuel for a 15 W fuel cell at the operation temperature of 30 °C or a ~30 W SOFC at 65 °C, assuming 50% fuel efficiency. Since BSCF had very low surface area (0.48 $m^2\ g^{-1}$) the improvement of the surface area of the catalyst by advanced synthesis technique could result in substantially increasing the catalytic activity. The BSCF catalyst operated stably for more than 10 h without failure. With the further modification of the catalyst via the strategy of doping, the catalyst could be in operation for hundreds of hours without degradation.

3.1. Fuel cell test

To test the fuel cell performance with the current in situ created gaseous H_2/NH_3 as fuels, an anode-supported thin-film electrolyte fuel cell based on ScSZ electrolyte was built with the configuration of NiO + ScSZ|ScSZ|LSM. Fig. 5 shows the typical microstructure of the single cell. As can be seen, the fuel cell had an electrolyte thickness of ~30 μm, cathode thickness of 35 μm, and anode thickness of ~1 mm. Porosity test demonstrated that the anode had a porosity of ~22 vol.% after reduction and the cathode of ~30 vol.%. Both the anode and cathode adhered to the electrolyte surfaces relatively well.

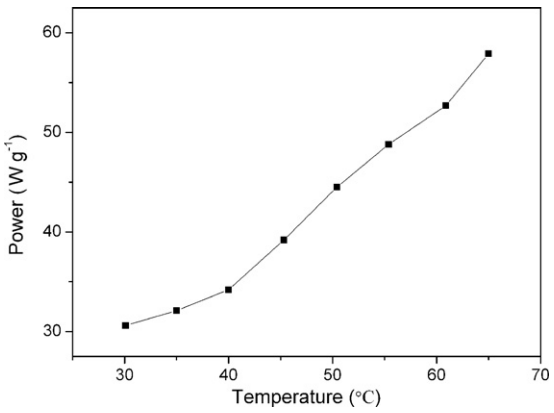

Fig. 4. The electrical energy produced by liquid hydrazine.

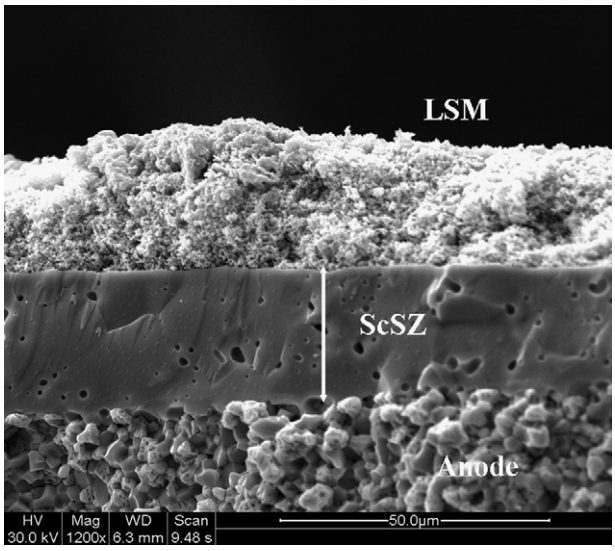

Fig. 5. The typical cross-sectional SEM image of a typical ScSZ + Ni supported thin-film ScSZ electrolyte solid-oxide fuel cell with LSM cathode.

For comparison, the fuel cell was first tested using pure hydrogen as the fuel. The corresponding *I–V* and *P–I* curves for the fuel cells are shown in Fig. 6a. An OCV of 1.12 V was reached at 900 °C. With the decrease of the operation temperature, the OCV increased steadily to 1.16 V at 650 °C. The OCVs were near the theoretical values, suggesting that no obvious gas leakage through the electrolyte membrane or sealing took place, which agrees well with no penetrated pin-holes observed in the electrolyte layer by SEM (Fig. 5). The power density decreased steadily with the decrease of operation temperature from ~1 W cm^{-2} at 900 °C, 412 mW cm^{-2} at 800 °C, to 67 mW cm^{-2} at 650 °C. The trend of decreased performance with the lowering of the operation temperature was attributed to the decrease of the cathode performance and the increase of the ohmic polarization from the electrolyte. After the test with hydrogen fuel, the in situ created H_2 and NH_3 from the catalytic decomposition of liquid-state N_2H_4 at 40 °C with 0.1 g catalyst were directed to the fuel cell as the fuels. Very good performance was also observed as shown in Fig. 6b. For example, a peak power density of 850 mW cm^{-2} and an OCV of 1.02 V were achieved at 900 °C, which is only slightly lower than that with hydrogen as the fuel. With decreasing operation temperature, the difference in peak power density between hydrogen fuel and in situ created H_2/NH_3 fuels became even smaller. A peak power density of 380 mW cm^{-2} was achieved at 800 °C with the fuels from the in situ catalytic decomposition of N_2H_4 at liquid state as compared to a value of 412 mW cm^{-2} with hydrogen as fuel. At the operation temperature of 650 °C, the performance is almost the same (71 mW cm^{-2} versus 67 mW cm^{-2}).

Fig. 7 shows the electrochemical impedance spectroscopy (EIS) of the fuel cell under open circuit voltages using H_2 and the in situ created NH_3 and H_2 as fuel(s) at various tempera-

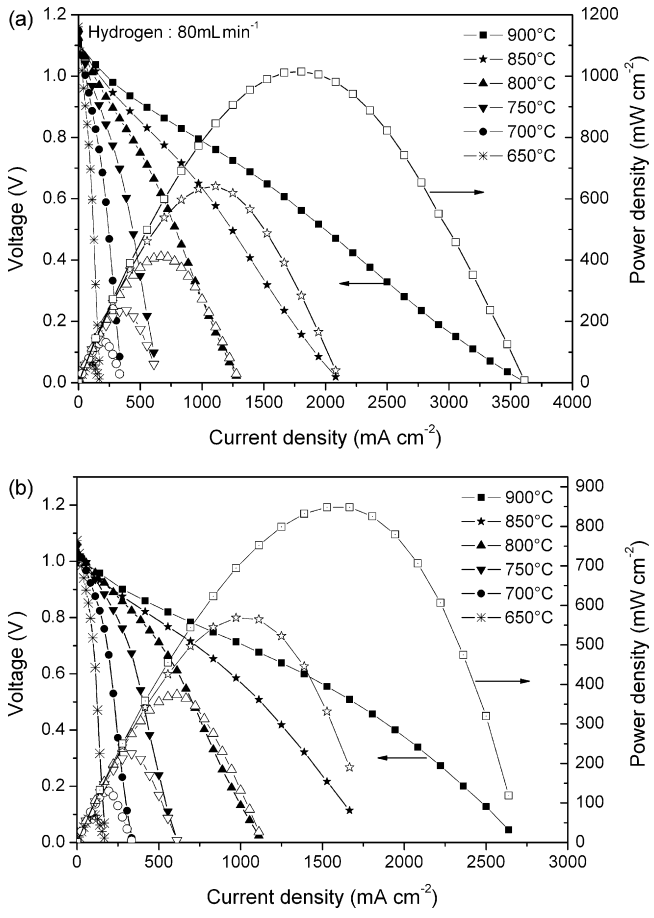

Fig. 6. The corresponding *I–V* and *I–P* curves of the NiO + ScSZ|ScSZ|LSM fuel cells with (a) H_2 as the fuel; (b) the in situ created H_2 and NH_3 as the fuels.

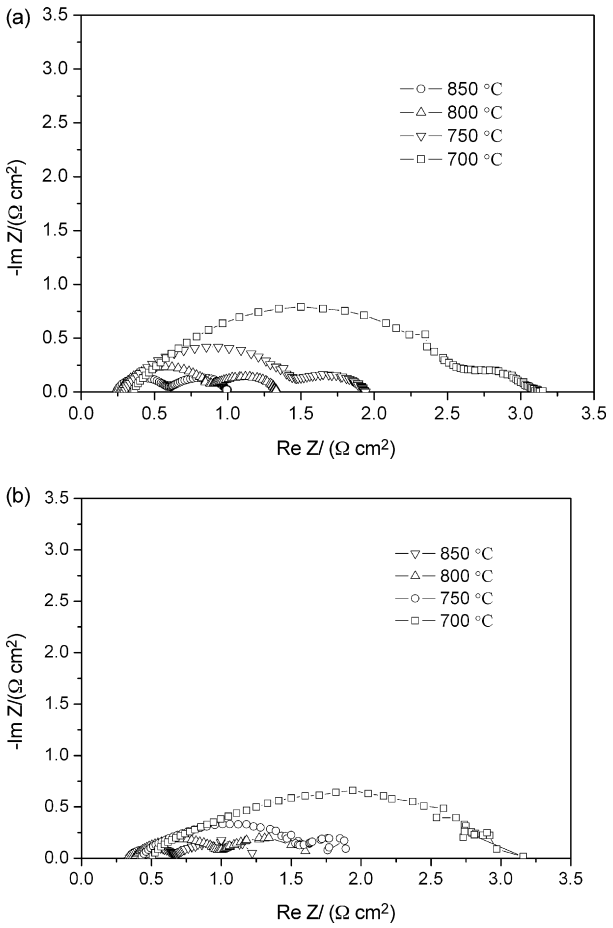

Fig. 7. The electrochemical impedance spectroscopy (EIS) of the fuel cell under open circuit voltages at various temperatures using (a) H_2 as fuel; (b) the in situ created NH_3 and H_2 as fuel(s).

tures, respectively. For both cases, it was found that the fuel cell polarization resistance was mainly contributed from the electrodes, especially at reduced temperatures. Such electrode polarization was mainly attributed to the poor activity of LSM cathode for oxygen reduction at reduced temperature. The development of innovative high performance cathode would expect a sharp increase in the fuel cell performance. The similar electrode polarization resistances with H_2 and in situ N_2H_4 decomposition product as fuel suggests that the similar anode overpotential, agreed well with the *I–V* polarization test.

Since the actual fuel for the SOFC in current hydrazine-fueled fuel cells is ammonia and small amounts of hydrogen, the direct electrochemical oxidation of NH_3 to N_2 and H_2O should demonstrate an increase in OCV with increase of temperature due to the positive absolute value of ΔG° for the following reaction:

$$4NH_3(g) + 6O^{2-} \rightarrow 6H_2O(g) + 2N_2(g) + 12e^- \quad (5)$$

$$O_2 + 4e^- \rightarrow 2O^{2-} \quad (6)$$

$$4NH_3(g) + 6O_2 \rightarrow 6H_2O(g) + 2N_2(g) \quad (7)$$

However, a decrease of OCVs with the increase of the operation temperature for the SOFC was observed operated on the in situ created H_2/NH_3, as shown in Fig. 6b, just as the same for hydrogen fuel. This suggests that the oxidation of NH_3 in current fuel cell systems is likely to proceed via the indirect way. First NH_3 was decomposed to N_2 and H_2 under the catalysts of the nickel anode:

$$2NH_3 \rightarrow N_2 + 3H_2 \quad (8)$$

Then H_2 was electrocatalytically oxidized to water and the simultaneous production of electricity:

$$H_2 + O^{2-} \rightarrow H_2O + 2e^- \quad (9)$$

Similar observations were noted by Meng and coworkers with ammonia as the fuel [34]. The typical anode material in SOFCs, nickel, is an excellent catalyst for ammonia decomposition. It was believed that ammonia could completely decompose over nickel anodes at temperatures as low as 600 °C [35]. Therefore, under current operation conditions, the direct fuel for the electrocatalytic oxidation over the anode is actually hydrogen instead of ammonia. It then well explained the similar performance of fuel cells with hydrogen fuel and the in situ created H_2/NH_3 fuel. The relatively lower OCVs for the fuel cell when operated on H_2/NH_3 than on H_2 is attributed to the dilution effect of nitrogen. Stable performance was observed during tens of hours' test. No morphologic change of the fuel cell was observed after the test using in situ created NH_3 and H_2 as the fuels.

Recently, it has been demonstrated that ammonia is an excellent fuel for SOFC [34,36–39]. The hydrazine could be treated as a liquid storage material for ammonia. It was reported that the reduction process of NiO in ammonia was too slow below 750 °C [34]. The availability of H_2 in the evolved gases from the catalytic decomposition of N_2H_4 over BSCF catalyst is then beneficial for operation at reduced temperatures, which allows the fuel cell anode no necessary to be pre-reduced even at a temperature lower than 600 °C.

Up until now, typically two types of liquid fuels were available for portable fuel cell application, *i.e.*, the fuel in liquid phase at room temperature and ambient pressure (such as ethanol), and pressurized liquid fuels such as NH_3 and liquefied petroleum gas (LPG). Fuel pumps and vaporization systems are needed to introduce the non-pressurized liquid fuel into the fuel cell reactor, while a high-pressure tank and gas value are needed for the storing and delivering of the pressurized liquid fuel. For both cases, the auxiliary components increase the complexity of the fuel cell system, which decreases the portability of the fuel cells. With the current in situ catalytic decomposition of liquid N_2H_4 to H_2 and NH_3, no gas valve, pressured tank or vaporization system is needed. Therefore the fuel cell system can be greatly simplified and constructed to be more compact. In addition, hydrazine has excellent handling characteristics, relatively high stability under normal conditions, clean decomposition products and high energy density. Its hydrogen percentage reaches as high as 12.5 wt.%, which is higher than all the available metal hydrides, in addition to other chemical hydrogen storage materials such as $NaBH_4$. It also has an excellent volumetric energy density of 63 mol H_2/L, which is higher than the liquid NH_3 value of 53 mol H_2/L, and methanol with a value of 49 mol H_2/L. N_2H_4 is in liquid state between a wide temperature range of 2.0–113.5 °C. It is miscible with water, methyl isobutyl alcohol. By forming the mixed solution, the temperature window of the liquid phase can be further widened. For example, when N_2H_4 combines with water to form hydrazine hydrate ($N_2H_4{\cdot}H_2O$), its melting point decreases to −51.5 °C and its boiling point increases to 120.1 °C. Although N_2H_4 is naturally toxic, it has a low vapor pressure of only 14.4 Torr at 25 °C, and therefore it is easy to be stored safely. More importantly, the complete decomposition products (N_2 and H_2), and the complete oxidation products (N_2 and H_2O) are not harmful. The in situ decomposition of N_2H_4 as fuel suggests that the actual fuels that were introduced into the fuel cell were N_2, H_2 and NH_3. Although it might be a minor amount of N_2H_4 present in the decomposed gas, N_2H_4 would be 100% thermally decomposed at a temperature higher than 250 °C, which further reduces the risk of exposing N_2H_4 to the environment. All of the above features make N_2H_4 the ideal fuel for portable SOFC applications.

4. Conclusions

Hydrazine was applied as the fuel for a SOFC with a typical nickel based anode. $Ba_{0.5}Sr_{0.5}Co_{0.8}Fe_{0.2}O_{3-\delta}$ oxide was found to be an active catalyst for the decomposition of N_2H_4 at liquid state to gaseous NH_3 and H_2 at room temperature and ambient pressure. Hydrogen selectivity as high as 10% was reached, suggesting that BSCF favored both the cracking of N–H and N–N bonds in N_2H_4. The in situ created products were found to be highly promising fuel for the SOFC and delivered a performance similar to using a hydrogen fuel. The combined advantages of the high energy density of N_2H_4 with the freedom from pressurized gas tanks and valves make N_2H_4 highly attractive for portable SOFC applications.

Acknowledgements

This work was supported by the National Natural Science Foundation of China under contract nos. 20646002, 20676061 and 20703024, and National Basic Research Program of China under contract no. 2007CB209704.

References

[1] N.Q. Minh, J. Am. Ceram. Soc. 76 (1993) 563–588.
[2] B.C.H. Steele, A. Heinzel, Nature 414 (2001) 345–352.
[3] T. Hibino, A. Hashimoto, T. Inoue, J. Tokuno, S. Yoshida, M. Sano, Science 288 (2000) 2031–2033.
[4] Z.P. Shao, J. Mederos, W.C. Chueh, S.M. Haile, J. Power Sources 162 (2006) 589–596.
[5] Z.P. Shao, S.M. Haile, J. Ahn, P.D. Ronney, Z.L. Zhan, S.A. Barnett, Nature 435 (2005) 795–798.
[6] M. Yano, A. Tomita, M. Sano, T. Hibino, Solid State Ionics 177 (2007) 3351–3359.
[7] X. Jacques-Bedard, T.W. Napporn, R. Roberge, M. Meunier, J. Power Sources 153 (2006) 108–113.
[8] N.M. Sammes, Y. Du, R. Bove, J. Power Sources 145 (2005) 428–434.
[9] T. Suzuki, T. Yamaguchi, Y. Fujishiro, M. Awano, J. Power Sources 160 (2006) 73–77.
[10] Y. Funahashi, T. Shimamori, T. Suzuki, Y. Fuishiro, M. Awano, J. Power Sources 163 (2007) 731–736.
[11] G.J. Saunders, J. Preece, K. Kendall, J. Power Sources 131 (2004) 23–26.
[12] W. Jamsak, S. Assaburnrungrat, P.L. Douglas, N. Laosiripojana, R. Suwanwarangkul, S. Charojrochkul, E. Croiset, Chem. Eng. J. 133 (2007) 187–194.
[13] Y. Inui, A. Urata, N. Ito, T. Nakajima, T. Tanaka, Energy Convers. Manage. 47 (2006) 1738–1747.
[14] K. Kendall, M. Slinn, J. Preece, J. Power Sources 157 (2006) 750–753.
[15] Z.F. Zhou, C. Gallo, M.B. Pague, H. Schobert, S.N. Lvov, J. Power Sources 133 (2004) 181–187.
[16] C. Lu, S. An, W.L. Worrel, J.M. Vohs, R.J. Gorte, Solid State Ionics 175 (2004) 47–50.
[17] S. McIntosh, R.J. Gorte, Chem. Rev. 104 (2004) 4845–4865.
[18] R.J. Gorte, J.M. Vohs, J. Catal. 216 (2003) 477–486.
[19] A. Atkinson, S. Barnett, R.J. Gorte, J.T.S. Irvine, A.J. Mcevoy, M. Mogensen, S.C. Singhal, J. Vohs, Nat. Mater. 3 (2004) 17–27.
[20] S.D. Park, J.M. Vohs, R.J. Gorte, Nature 404 (2000) 265–267.
[21] S.W. Tao, J.T.S. Irvine, Nat. Mater. 2 (2003) 320–323.
[22] M.R. Andrew, W.J. Gressler, J.K. Johnson, R.T. Short, K.R. Williams, J. Appl. Electrochem. 2 (1972) 327–336.
[23] S.G. Meibuhr, J. Electrochem. Soc. 121 (1974) 1264–1270.
[24] K. Tamura, T. Kahara, J. Electrochem. Soc. 123 (1976) 776–780.
[25] K. Yamada, K. Yasuda, N. Fujiwara, Z. Siroma, H. Tanaka, Y. Miyazaki, T. Kobayashi, Electrochem. Commun. 5 (2003) 892–896.
[26] K. Yamada, K. Asazawa, K. Yasuda, T. Ioroi, H. Tanaka, Y. Miyazaki, T. Kobayashi, J. Power Sources 115 (2003) 236–242.
[27] K. Yamada, K. Yasuda, H. Tanada, Y. Miyazaki, T. Kobayashi, J. Power Sources 122 (2003) 132–137.
[28] W. Zhou, Z.P. Shao, W.Q. Jin, J. Alloys Compd. 426 (2006) 368–374.
[29] Z.P. Shao, W.S. Yang, Y. Cong, H. Dong, J.H. Tong, G.X. Xiong, J. Membr. Sci. 172 (2000) 177–188.
[30] Z.P. Shao, S.M. Haile, Nature 431 (2004) 170–173.

[31] W. Zhou, X.P. Xue, L. Ge, Y. Zheng, Z.P. Shao, W.Q. Jin, J. Inorg. Mater. 22 (2007) 657–662.
[32] M.Y. Zheng, R.H. Cheng, X.W. Chen, N. Li, L. Li, X.D. Wang, T. Zhang, Int. J. Hydrogen Energy 30 (2005) 1081–1089.
[33] X.W. Chen, T. Zhang, M.Y. Zheng, Z.L. Wu, W.C. Wu, C. Li, J. Catal. 224 (2004) 473–478.
[34] Q.L. Ma, J.J. Ma, S. Zhou, R.Q. Yan, J.F. Gao, G.Y. Meng, J. Power Sources 164 (2007) 86–89.
[35] J. Staniforth, R.M. Ormerod, Green Chem. 5 (2003) 606–609.
[36] Q.L. Ma, R.R. Peng, L.Z. Tian, G.Y. Meng, Electrochem. Commun. 8 (2006) 1791–1795.
[37] A. Wojcik, H. Middleton, I. Damopoulos, J.V. Herle, J. Power Sources 118 (2003) 342–348.
[38] Q.L. Ma, R.R. Peng, Y.J. Lin, J.F. Gao, G.Y. Meng, J. Power Sources 161 (2006) 95–98.
[39] K. Xie, Q.L. Ma, B. Lin, Y.Z. Jiang, J.F. Gao, X.Q. Liu, G.Y. Meng, J. Power Sources 170 (2007) 38–41.